BRNO UNIVERSITY OF TECHNOLOGY
VYSOKÉ UČENÍ TECHNICKÉ V BRNĚ

CENTRAL EUROPEAN INSTITUTE OF TECHNOLOGY BUT
STŘEDOEVROPSKÝ TECHNOLOGICKÝ INSTITUT VUT

STRUCTURE AND PROPERTIES OF HYDROXYAPATITE-MAGNESIUM COMPOSITES PRODUCED BY THE MEANS OF CURRENT ASSISTED INFILTRATION SINTERING

STRUKTURA A VLASTNOSTI KOMPOZITŮ NA BÁZI HYDROXYAPATITU A HOŘČÍKU, PŘIPRAVOVANÝCH METODOU PROUDEM ASISTOVANÉ SLINOVACÍ INFILTRACE

SHORT VERSION OF DOCTORAL THESIS
TEZE DIZERTAČNÍ PRÁCE

AUTHOR
AUTOR PRÁCE
Mariano Casas Luna

SUPERVISOR
ŠKOLITEL
doc. Ing. Ladislav Čelko, Ph.D.

BRNO 2020

KEYWORDS:

Magnesium, Hydroxyapatite, tricalcium phosphate, interpenetrated composites, Mechanical properties, Corrosion behaviour, Cytotoxicity.

Klíčová Slova:
Hořčík, Hydroxyapatit, trikalciumfosfát, interpenetratované kompozity, mechanické vlastnosti, korozní chování, cytotoxicita.

BIBLIOGRAPHIC CITATION:

Casas-Luna, M. *Structure and properties of hydroxyapatite – magnesium composites produced by means of current-assisted infiltration sintering.* Brno: Brno University of Technology, Central European Institute of Technology, 2020. 28 p. Dissertation supervisor: Assoc. Prof. Ladislav Čelko, Ph.D.

Biblografická Citace:
Casas-Luna, M. *Struktura a vlastnosti kompozitů na bázi hydroxyapatitu a hořčíku, připravovaných metodou proudem asistované slinovací infiltrace*. Brno: Vysoké učení technické v Brně, Středoevropský technologický institut VUT, 2020. 28 stran. Vedoucí práce docent Ladislav Čelko, Ph.D.

SWORN STATEMENT

I hereby declare that I have written the PhD thesis on my own according to advice of my supervisor Assoc. Prof. Ladislav Čelko and that all the literary sources are quoted correctly and completely. This dissertation thesis is the property of the Central European Institute of Technology (CEITEC), Brno University of Technology (BUT), Czech Republic and it can be used for commercial purposes only with consent of the doctoral thesis supervisor and the director of CEITEC, BUT.

Čestné prohlášení
Tímto prohlašuji, že jsem vypracoval doktorskou práci sám, dle doporučení vedoucího Assoc. Prof. Ladislav Čelko a že všechny literární zdroje jsou citovány správně a úplně. Tato disertační práce je majetkem Středoevropského technologického institutu (CEITEC), VUT v Brně a může být použita ke komerčním účelům pouze se souhlasem vedoucího disertační práce a ředitele CEITEC VUT v Brně.

Mariano Casas Luna

ABSTRACT

Magnesium and calcium phosphate composites are promising materials to create biodegradable and load-bearing implants for bone regeneration. The present work is focused on the design, processing and characterization of interpenetrated magnesium / calcium phosphate (Mg/CaP) composites. Calcium phosphates such as, hydroxyapatite (HA), calcium-deficient HA (CDHA) and tricalcium phosphate (TCP) were synthetized and used for the production of controlled porous scaffolds by means of robocasting technique. The final porous preforms with an orthogonal grid arrangement and internal macro-pores of ~500 µm were obtained and sintered at 1100 ºC for 5 h. The Mg/CaP interpenetrated composites were obtained by infiltrating the porous ceramic scaffolds with pure Mg and Mg alloys containing low amounts of calcium or zinc, i.e. Mg – 0.2 wt.% Ca and Mg – 1 wt.% Zn. The infiltration was carried out using a here-developed and recently introduced technique referred to as Current-Assisted Metal Infiltration (CAMI). The CAMI methodology allowed the infiltration of porous ceramic preforms with a molten metal in less than 15 minutes. Fast melting and final solidification of the Mg/CaP composites was achieved with the assistance of pulsed electrical current. The final interpenetrated composites were physicochemically characterised by means of scanning electron microscopy, X-ray computed micro-tomography, X-ray diffraction and optical microscopy in order to determine the phase distribution and the interaction between the materials. In addition, the mechanical resistance under compression, the degradation rate by different techniques, and the biocompatibility of the produced composites were evaluated in an attempt to introduce these types of materials as potential degradable biomaterials for use in the manufacturing of plates and/or screws for orthopaedics.

Abstrakt

Hořčík a kompozity fosforečnanu vápenatého jsou slibnými materiály pro biodegradabilní a nosné implantáty určené pro regeneraci kostí. Předložená práce je zaměřena na návrh, zpracování a charakterizaci vnitřně propojených kompozitů hořčíku s fosforečnanem vápenatým (Mg/CaP). Fosforečnany vápenaté jako jsou hydroxyapatit (HA), kalcium-deficitní hydroxyapatit (CDHA) a fosforečnan vápenatý (TCP) byly syntetizovány a použity pro výrobu skafoldů s kontrolovanou porozitou pomocí metody robocastingu. Byly připraveny porézní předlisky s ortogonální mřížkou a s vnitřními makropóry o velikosti ~500 µm, které byly následně slinovány za teploty 1100 °C po dobu 5 hodin. Vnitřně propojené Mg/CaP kompozity byly připraveny infiltrací čistého hořčíku a hořčíkových slitin obsahujících malá množství vápníku nebo zinku, například 0,2 hm.% vápníku a 1 hm.% zinku do porézních keramických skafoldů. Infiltrace byla provedena pomocí námi vyvinuté a nově popsané metody známé jako "Proudem asistovaná slinovací infiltrace" (z angl. Current Assisted Metal Infiltration (CAMI)). CAMI metoda umožňuje do 15 minut infiltrovat porézní keramický předlisek roztaveným kovem. Pulzujícím elektrickým proudem bylo dosaženo rychlého tavení a následného tuhnutí Mg/CaP kompozitů. Fyzikálně-chemické vlastnosti finálních vnitřně propojených kompozitů byly stanoveny pomocí rastrovací elektronové mikroskopie, počítačové mikro-tomografie, rentgenové difrakční analýzy a optické mikroskopie za účelem stanovení fázové distribuce a interakce mezi materiály. Kromě toho byla u připravených kompozitů hodnocena jejich mechanická pevnost v tlaku, degradační rychlost pomocí různých metod a biokompatibilita spolu s pokusem o uvedení těchto typů materiálů jako potenciálních degradabilních biomateriálů určených pro výrobu desek a/nebo šroubů pro ortopedické aplikace.

CONTENTS

1. INTRODUCTION

Bone degenerative problems besides numerous bone fractures, osteoporosis, and other musculoskeletal problems are affecting millions of people worldwide and they need to be solved by using permanent or temporary implants. The number of new fractures in 2010 in the EU was estimated at 3.5 million, expecting a rise of 28% by 2025. Only in the Czech Republic, approximately 72,000 fractures were reported in 2010, representing an average economic burden of € 273 million each year [1]. From this point of view, the design and study of new materials for orthopaedic applications are of high interest for the industry and the research field, with the aim to increase the quality of life among afflicted people.

Up to now, a wide range of materials have been used for bone repairs. Metallic devices are usually implanted for load bearing applications while ceramics and polymers are mostly used as bioactive and degradable materials, respectively. Recently, new types of advanced composites have appeared because of their unique properties inside the human body, combining bioactivity with adjusted mechanical behaviour.

Calcium phosphates (CaP's) such as hydroxyapatite (HA), calcium-deficient hydroxyapatite (CDHA) and tricalcium phosphates (α-TCP or β-TCP) are the most commonly used materials for bioactive implants due to their chemical composition, which is similar to the inorganic phase of the natural bone. This chemical composition similarity gives them good biocompatibility. However, the ceramic nature of CaP's makes them possess low ductility and fragile behaviour, impeding their application in the treatment of bone defects under load-bearing conditions. Consequently, metallic and CaP degradable composites are gaining attraction for the fabrication of osteosynthetic implants [2,3]. The driving force is the effort to increase the mechanical strength of CaP's, without sacrificing its degradability and osteoconductivity [4]. Among the different degradable metals available, magnesium (Mg) appears to be one of the best alternatives due to its good tolerance in the human body, its osteogenic effect, and mechanical properties similar to the human bone [5].

Composites and functionally graded materials (FGM's) consisting of Mg and CaP are a promising solution to yield bioactive/degradable implants in orthopaedics. Different methods have been developed to produce Magnesium - Calcium phosphate (Mg/CaP) composites [6,7].

In the present work, the synthesis and production of functionally interpenetrated materials based on CaP (such as HA and TCP) and Mg alloys (i.e. Mg-Ca and Mg-Zn) was performed. Robocasting was used to build cylindrical CaP scaffolds with interconnected pores of ~500 μm. Later, scaffolds of ~8 mm in diameter and ~10 mm in height were successfully infiltrated by Mg or Mg alloys to obtain the interpenetrated Mg/CaP composites. At the same time, a new pressureless infiltration method was explored and implemented in the study. The process referred to as current-assisted metal infiltration (CAMI) uses the principle of spark plasma sintering [8] to melt magnesium under vacuum, and once it is in the liquid state, infiltrate the bioceramic preform by gravity and vacuum suction. Finally, the chemical and the structural characterizations of the interpenetrated composites were performed and their degradation rate and cytotoxicity response were calculated under simulated physiological conditions as an initial attempt to use these composites as resorbable biomaterials for orthopaedic applications.

2. LITERATURE REVIEW

2.1. DEGRADABLE BIOMATERIALS

The study and design of degradable biomaterials has become one of the most revolutionary research topics at the forefront of the biomaterials field. This novel class of biomaterials are expected to be used as implants to fulfil a temporary function. The use of temporary implants is necessary in clinical cases where the implant covers the function of the surrounding living tissue while the body regenerates and heals [9]. The use of degradable implants is important in some orthopaedic and cardiovascular applications where the implant must be removed after the healing of the damaged tissue, involving a second surgery, which implies personal, medical, social, and economic consequences. All such complications can be solved by the development of degradable biomaterials with controlled degradation rate inside the human body.

An ideal degradable material should exhibit bioactivity while the degradation rate is in accordance with the healing time without compromising the mechanical requirements during the process. In addition, the corrosion/degradation products must be inert – not toxic – in the human body [2,10]. Thus, depending on the tissue being reabsorbed and regenerated, degradable polymers, ceramics or even metals can be used.

In the case of bone regeneration, avoiding a second surgery to remove implants like plates or screws is of high importance since it reduces the risk to both the specialist and the patient. In these terms, degradable polymers are mostly limited to low load-bearing applications due to their scarce mechanical properties, and in this field the degradable ceramics or metals fulfil this requirement and extend the possibilities for the development of a next generation of degradable and bioactive implants for orthopaedics.

The most studied ceramics in orthopaedics are the family of calcium phosphates due to their very well-known bioactivity, mostly osteoconductivity, which is a product of their chemical composition, similar to the inorganic phase of bones. In the case of metals, even though they exhibit excellent mechanical properties with more ductility response than ceramics, the selection of the material is limited to the biocompatibility properties.

2.2. BIOABSORBABLE CALCIUM PHOSPHATES (CAP) AS ORTHOPAEDIC MATERIALS

Calcium phosphates belong to the group of bioactive ceramics that can trigger bone regeneration due to their chemical composition, similar to the natural bone. These bioceramics promote osteoinduction and osteoconduction by the interaction with the bone cells that leads to the reabsorption of these ceramics and their transformation into natural bone [4]. Osteoinduction is the process by which osteogenesis – bone regeneration – is induced and it happens during any type of bone healing [11]. On the other hand, osteoconduction is the process that involves the active surface of a material that is in contact with the bone tissue and promotes the growing of bone tissue on the surface of the material [12].

Among the most widely used CaP in orthopaedics and dentistry, hydroxyapatite – HA, $Ca_{10}(PO_4)_6(OH)_2$ – is the most renowned one and it has been tested as artificial bone since its chemical composition and structure are linked to the inorganic phase of the natural bone. When stoichiometric HA is deficient in calcium, known as calcium-deficient hydroxyapatite (CDHA, $Ca_9(HPO_4)(PO_4)_5(OH)$), the compound is more favourable as bone graft because it has a faster dissolution rate under physiological

conditions than stoichiometric HA has. Additionally, CDHA has a higher osteoconduction, enabling fast bonding and interaction with the bone cells [13].

Another widely used resorbable CaP is the tricalcium phosphate (TCP, $Ca_3(PO_4)_2$). TCP exists in the form of three crystalline structures: monoclinic or α-TCP, hexagonal or α'-TCP (not stable at room temperature), and rhombohedral or β-TCP. The monoclinic and hexagonal phases are stable at high temperatures, above 1150 ºC and >1430 ºC, respectively [14]. However, an abrupt quenching of the ceramic can preserve the α-TCP at room temperature as a metastable phase. TCP polymorphs differ significantly in their crystalline structure, consequently in their density and solubility. Then, α-TCP presents faster resorption due to the rapid hydrolysis to CDHA [14].

The biological response *in vivo*, as the resorption rate of the CaP, is a function of the chemical composition, crystallographic structure and microstructural morphology of these bioceramics. Under physiological conditions, i.e. pH = 7.2 – 7.4, the concentration of dissolved Ca and P from the here-mentioned CaP's decreases in the following order: α-TCP > β-TCP > CDHA > HA [15]. Under these conditions, HA is the most stable phase and therefore it is the main precipitation product during the biodegradation and mineralization of the CaP bioceramics.

2.3. MAGNESIUM AND ITS ALLOYS AS DEGRADABLE BIOMATERIALS FOR ORTHOPAEDIC APPLICATIONS

Magnesium (Mg) and its alloys have attracted attention as potential degradable materials for bone regeneration. Magnesium is an exceptional lightweight metal with a density of 1.74 $g \cdot cm^{-3}$. The fracture toughness of magnesium is higher in comparison with ceramic biomaterials such as HA or any other CaP present in the human bones, while the elastic modulus is close to that of bone, i.e. 40 GPa compared to ~20 GPa, respectively [16]. The main drawback of magnesium that limits its medical application is its high corrosion rate under physiological conditions, losing mechanical integrity before the tissue can be sufficiently healed. Additionally, the corrosion of Mg and its alloys produces hydrogen at a fast rate, which is not favourable for the host tissue and the healing process.

However, there are some possibilities of tailoring the corrosion rate of Mg under physiological conditions, most frequently by alloying the Mg with non-toxic elements such as calcium, manganese and zinc; or using protective coatings, usually based on calcium phosphate bioceramics [16,17]. There are three main considerations for the selection of the alloying element in degradable Mg-alloy biomaterials. The first and most important is the nontoxicity of both the alloying element and the corrosion products. The second consideration is the influence of the alloying element on the corrosion behaviour of the alloy. This factor is important when tailoring the degradation rate of the material; due to the low electrochemical potential of Mg (-2.37 V), if the alloy is not in solid solution, intermetallic phases are formed that induce the internal galvanic corrosion and decrease the corrosion resistance of the material. And the last main consideration is the effect on the mechanical properties of the alloy.

For the design of non-toxic Mg alloys, the chemical elements are limited to Ca, Zn, Si, Gd, Zr, Sr and Y [18,19]. The reasons are mainly based on the mechanical properties, bioactivity and degradation speed assays. Calcium, zinc and rare-earth metals are the group of the most frequently studied alloying elements for Mg.

To date, numerous Mg-based degradable biometals have been tested for bone regeneration in order to characterise their corrosion and tissue response. Most of the investigated alloys indicate good biocompatibility after in *in-vivo* tests, showing that Mg-based alloys can promote the formation of new bone around the implanted material. Additionally, the corrosion products reveal high deposition of CaP minerals, showing in some cases good contact between the implant and the adjacent bone. Nevertheless, the main drawback regarding the gas cavity presence is still observed in almost all the studies. The hydrogen production is usually higher in the initial post-implantation period and gradually decreases with time due to surface passivation of the implant [20].

2.4. ROBOCASTING OF POROUS CONTROLLED SCAFFOLDS

Due to its simplicity, robocasting, also known as direct ink writing (DIW), is one of the widely-used additive manufacturing technologies for the processing of biomaterials structures, bioceramics in particular. The technique is based on the direct extrusion of an ink, which is mainly composed of an injectable paste or slurry of the processed material. The process was developed at Sandia National Laboratories in 1997 as a method for rapid prototyping and free-forming objects with low-binder slurry following a computed design [21]. In more detail, robocasting is the robotic deposition of highly concentrated suspensions or pastes, between 50 to 65 vol.% of a powder in a solvent (typically water) with an organic additive or binder in order to provide good rheological properties, making it possible to construct a computed-design structure following a desired pattern on a layer-wise deposition [22]. After robocasting, the 3D object must be sintered to consolidate the powder particles and burn out the solvent and binder in order to obtain the final dense structure. Thus, the robocasting technique allows the design and rapid fabrication of bioceramic materials in complex 3D shapes without the need for expensive tooling. Calcium phosphate structures with controlled interconnected porosity for cell seeding have recently been produced by this technology. They have shown excellent bioactive properties due to the microstructure and chemical composition but with the main drawback of poor mechanical properties due to the high porosity of the bodies, which is not suitable for load-bearing applications [23,24].

2.5. LIQUID METAL INFILTRATION: MANUFACTURING OF INTERPENETRATED COMPOSITES

Liquid metal infiltration of ceramic preforms is one of the best-suited fabrication methods for the production of matrix-based graded composites with a variety of complex shapes having control over the volume fraction of the embedded materials. The metal infiltration procedure consists in a liquid-state fabrication method, in which a porous preform (usually as reinforcement) in the form of ceramic particles, fibres, or interconnected porous bodies, are embedded in a molten metal, which fills the porosity between the dispersed-phase material [25].

The liquid infiltration processes can be classified in two categories: i) spontaneous infiltration, and ii) forced infiltration. This classification depends on the wettability between the liquid component and the solid material to be infiltrated. Therefore, when the capillary action of the solid material acts as the driving force for the infiltration, then the process occurs spontaneously. On the other hand, when an external force such as gas pressure, mechanical pressure, squeeze, electromagnetic field, etc. is needed to make the liquid enter the pores of the solid material, then the process is considered as forced infiltration [26].

The fabrication of interpenetrated materials can be successfully and easily performed by liquid infiltration. The interpenetrated composites can be classified according to the distribution of their phases

along the volume in: i) randomly distributed or ii) well-ordered interpenetrated composites. Typically, the open porosity distribution and pore geometry are difficult to control when using free particles, fibres or porous bodies; however, with additive manufacturing, the fabrication of patterned pores is not a terminating issue when making of controlled interpenetrated composites.

2.5.1. CURRENT-ASSISTED METAL INFILTRATION (CAMI)

A novel and rapid infiltration method has lately been developed and introduced for the processing of interpenetrated composites where one of the phases, in principle metallic, is melted to fill the open porosity of a foam, which is usually ceramic-based. The infiltration technique combines the melting of the metallic phase by an electric current flux and the mechanical pressing of the system by a set of punches in a graphite die.

The current-activated and pressure-assisted infiltration can be seen as an extension of the spark plasma sintering technique, as the processing happens in a graphite mould under vacuum and the heating of the powder particles is based on the Joule heating effect generated by the electrical current circuit. From this extent, the versatility of this infiltration method can be mixed with a densification or sintering process, achieving a rapid consolidation of green structures and infiltration of porous structures for the manufacturing of interpenetrated composites [27].

Nevertheless, pressure-assisted methods cannot be used extensively for the infiltration of all preforms due to mechanical compressive resistance limitations, especially in ceramic foams that are very fragile. The redesign of the current-activated and pressure-assisted process was accomplished by the development of a new methodology that carries out the infiltration at the same time that the consolidation of the whole interpenetrated composite is taking place. The technique has been called current-assisted infiltration sintering (CAIS) because it has the same principle of heating by the Joule-effect, so the entire process is accomplished in a few minutes. A variant of the technique's name has been introduced, namely current-assisted metal infiltration (CAMI), considering that the sintering or consolidation happens when the infiltration process is taking place. The CAMI processing has been tested and proved for the infiltration of porous calcium-phosphate structures with molten magnesium and zinc [28,29].

2.6. MAGNESIUM / CALCIUM-PHOSPHATE (Mg/CaP) COMPOSITE BIOMATERIALS

A new generation of degradable biomaterials has been developed due to the need for more bioactivity and interaction of the implants with the surrounding tissues. Furthermore, the degradation behaviour is needed to avoid second surgeries, when it is necessary to remove the implants after the healing process. In this extent, magnesium (Mg) and its alloys are potential candidates because of their similar strength to the bone tissue and biocompatibility, compared to the available metallic implants [16,19]. Nevertheless, Mg corrodes rapidly under physiological conditions, losing its integrity and mechanical properties before the healing process is finished or sufficient for mechanical loading. Thus, Mg alloys have found their application in the fabrication of stents for atrophied arteries or for screws that are not under considerable mechanical stress [30]. However, the desire to expand the use of Mg alloys for load-bearing applications with controlled degradation rate is ongoing.

Recent findings have proved that the addition of ceramic reinforcement into Mg or its alloys can enhance the mechanical properties and corrosion resistance of the composites, compared to the bare metal.

The most promising composites are based on reinforcing bioceramic phases, of particular interest are the family of calcium phosphates (CaP's) due to their high bioactive properties and possible bioresorption [4].

Therefore, extensive investigations have been focussed on composites based on pure Mg or Mg alloys containing diverse quantities of calcium, zinc, and rare-earth elements in combination with various CaP's such as hydroxyapatite (HA), calcium polyphosphate (CPP), β-tricalcium phosphate (β-TCP) or their combination produced by different manufacturing processes, which mostly include powder metallurgy, stirred casting method, or liquid infiltration of porous preforms [31].

3. AIMS OF THE THESIS

The doctoral thesis is focused on the design and manufacture of interpenetrated magnesium/calcium-phosphate composites and their wide characterization as potential degradable biomaterials for orthopaedics.

In the study, hydroxyapatite, calcium-deficient hydroxyapatite and β-tricalcium phosphate were used for the fabrication of porous preforms by means of the robocasting technique in order to obtain a precise control of the porosity degree and pore geometry. The consolidated preforms were infiltrated with ultra-high pure Mg and Mg-X alloys (X = 0.2 wt. % Ca and 1 wt. % Zn) using the newly developed current-assisted metal infiltration (CAMI) technique.

The Mg/CaP interpenetrated composites were evaluated in terms of their microstructure, chemical composition, volumetric phase distribution, mechanical behaviour under compression, degradation behaviour in simulated physiological conditions, and *in vitro* test response.

The dissertation aim was accomplished fulfilling specific objectives linked to the following activities:

- Synthesis and processing of hydroxyapatite and tricalcium phosphate powders *via* soft chemistry routes and high-temperature treatment.
- Manufacture of controlled-porous scaffolds (preforms) using the robocasting technique.
- Consolidation and infiltration of bioceramic scaffolds with magnesium and magnesium alloys (containing calcium and zinc) using the current-assisted metal infiltration technique.
- Characterization of obtained interpenetrated composites using micro-computed tomography, X-ray diffraction and metallography observation by optical and scanning electron microscopy techniques.
- Evaluation of the mechanical properties by compression test of the produced Mg/CaP composites.
- Evaluation of the degradation rates under simulated physiological conditions of the produced Mg/CaP composites.
- Evaluation of the cytotoxicity response of the produced Mg/CaP composites.

4. MATERIALS AND METHODS

The dissertation topic was divided into several activities and tests in the frame of four subsequent stages: (i) synthesis of CaP and robocasting of controlled porous scaffolds; (ii) casting and measurement of corrosion behaviour of Mg alloys containing low amounts of calcium and zinc; (iii) infiltration of CaP scaffolds with pure Mg or Mg alloys using the CAMI technique; and (iv) physicochemical characterization of the composites produced and their mechanical and biocompatibility testing.

4.1. SYNTHESIS OF CALCIUM PHOSPHATES (CAP'S) AND PRODUCTION OF CONTROLLED POROUS SCAFFOLDS

4.1.1. SYNTHESIS OF HA, β-TCP AND CDHA POWDERS

Hydroxyapatite powder was synthesised through a chemical precipitation reaction between phosphoric acid and calcium hydroxide [4]. The synthesis follows the reaction:

$$5Ca(OH)_2 + 3H_3PO_4 \rightarrow Ca_5(PO_4)_3(OH) + 9H_2O \quad \textbf{(Eq. 1)}$$

In the same way, the β-TCP powder was synthesised. The synthesis consisted in the precipitation of CDHA with a Ca/P atomic ratio of close to 1.5. The reaction followed the chemical equation:

$$3Ca(OH)_2 + 2H_3PO_4 \rightarrow Ca_{10-x}(PO_4)_{6-x}(HPO_4)_x\,(OH)_{2-x} \quad \textbf{(Eq. 2)}$$

The CDHA decomposes at temperatures above 800 ºC to produce TCP; the decomposition follows the reaction [14,32]:

$$Ca_{10-x}(PO_4)_{6-x}(HPO_4)_x\,(OH)_{2-x} \rightarrow (1-x)Ca_{10}(PO_4)_6(OH)_2 + 3Ca_3(PO_4)_2 + xH_2O\uparrow \quad \textbf{(Eq. 3)}$$

For the synthesis of calcium-deficient hydroxyapatite (CDHA), tricalcium phosphate in its monoclinic phase (α-TCP) was produced by the high-temperature solid-state reaction between calcium carbonate and calcium hydrogen phosphate at 1400 ºC. The obtained α-TCP powder hydrates to precipitate CDHA crystals following the chemical reaction:

$$\alpha\text{-}Ca_3(PO_4)_2 + H_2O \rightarrow Ca_{10-x}(PO_4)_{6-x}(HPO_4)_x\,(OH)_{2-x}, \quad \textbf{(Eq. 4)}$$

where *x* is between 0 and 1, keeping an elemental Ca/P ratio of between 1.67 and 1.5.

4.1.2. DIRECT INK WRITING OF CALCIUM-PHOSPHATE INJECTABLE PASTES

A set of macro-porous cylindrical structures were produced by robocasting injectable bioceramics. Injectable paste of commercial β-tricalcium phosphate (VWR, Belgium) was obtained by mixing the commercial powder with a 40 wt. % Pluronic F-127 (Sigma-Aldrich, Germany) solution in distilled water. A liquid-to-powder ratio was set at 0.6 gram of Pluronic solution per each gram of commercial β-TCP powder.

The initial porous cylinders were produced with nominal pore sizes of 150, 350, 500 and 1000 µm. The effect of the pore size on the infiltration success was evaluated. After this preliminary analysis, the fabrication of injectable pastes from synthesised HA, β-TCP and α-TCP powders was carried out for the

robocasting of porous cylindrical scaffolds of 10 mm in diameter and 10 mm in height with a macro-pore size of ~500 µm and using a nominal aperture size of 410 µm.

The sintering of HA and β-TCP scaffolds were set at 1200 ºC for 5 h. For the consolidation (hardening) of CDHA scaffolds, the hydration reaction of the α-TCP scaffolds was carried out by storing the robocast structures at 37 ºC in 100% humid atmosphere for 24 h and afterwards immersed in distilled water at 37 ºC for 6 days to complete the hydrolysis of the TCP polymorph into calcium-deficient hydroxyapatite (**Eq. 4**).

4.2. MANUFACTURING BY INDIRECT CHILL CASTING OF Mg ALLOYS

Ultra-high purity magnesium was used for the production of two degradable Mg alloys by the indirect chill casting method. Firstly, blocks of pure Mg were melted at 670 ºC using an electronic resistance furnace under a protective atmosphere of Ar with 2 vol. % of SF_6.

The nominal calcium content for the Mg-Ca alloys was set at 0.2, 0.4, 0.6 and 0.8. wt. %, while for the Mg-Zn alloys, the nominal content of zinc was 1, 2 and 3 wt. %. The alloys were annealed at 400 ºC for 2 h and hot-extruded at 300 ºC to obtain bars of 1 cm in diameter.

The chemical composition of the alloys was determined by X-ray fluorescence (Spectrolab M9, Spectro-Ametek-Klave, Germany) and in the case of the calcium concentration, it was estimated by atomic absorption spectroscopy. Finally, the degradation behaviour of as-extruded alloys was evaluated in simulated body fluid (SBF) at 37 ºC. From the results, the best two corrosion resistant alloys were selected for the infiltration of the CaP scaffolds.

4.3. MAGNESIUM INFILTRATION OF CaP SCAFFOLDS BY CURRENT-ASSISTED METAL INFILTRATION (CAMI)

Robocast CaP scaffolds were used as preforms for the liquid metal infiltration with pure Mg, Mg alloy containing 0.2 wt. % of Ca, and Mg alloy with 1 wt. % of Zn (alloys that revealed the best corrosion resistance) by means of the CAMI technique. Mg and Mg alloys discs of 10 mm in diameter and 10 mm in height were used for the infiltration of CaP preforms. **Figure 1** shows the design of the CAMI die and the initial arrangement of the preform and metallic disc for carrying out the infiltration process for the manufacturing of the interpenetrated Mg/CaP composites.

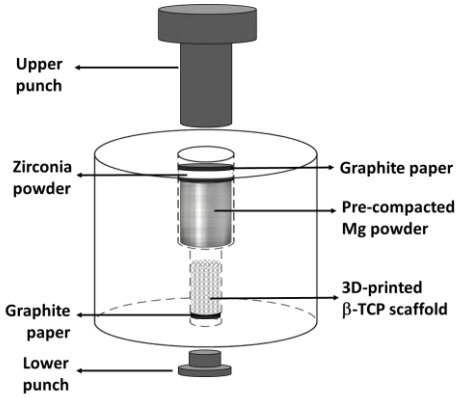

Figure 1. Graphite-die design and initial arrangement for the current-assisted metal infiltration technique.

The infiltration of magnesium was performed in a spark plasma sintering apparatus (SPS, Dr. Sinter 1050, Japan). The melting of magnesium and the infiltration were achieved by heating up the die, reaching a temperature of 670 ºC with a heating ramp of 100 ºC·min^{-1}. The set of interpenetrated Mg/CaP composite samples is listed in **Table 1**.

Table 1. Number of interpenetrated Mg/CaP composites produced by the infiltration of CaP preforms with pure Mg and Mg alloys.

Bioceramic preform	Infiltrating alloy		
	Pure Mg	Mg-0.2%Ca	Mg-1%Zn
HA	15	15	-
CDHA	15	15	15
β-TCP	15	15	-

4.4. CHARACTERIZATION OF Mg ALLOYS AND Mg/CaP INTERPENETRATED COMPOSITES

The physicochemical characterization of pure alloys and interpenetrated composites was performed using micro-computed tomography (μCT), optical microscopy (OM), scanning electron microscopy (SEM) and X-ray diffraction (XRD).

Regarding the mechanical properties of the Mg/CaP composites, the compressive strength, yield strength and maximum strain of the materials at the uniaxial compression test were measured. The degradation kinetics were assayed using a conventional simulated body fluid for 2 weeks at 37 ºC by H_2 evolution and potentiodynamic measurements. Similarly, the toxicity of the final materials was analysed during the first 6 days using SAOS-2 cells.

All the mechanical tests, degradation behaviour and cytocompatibility assays were performed for each type of material in triplicates. The statistical differences between the interpenetrated Mg/CaP composites were determined using the *t*-student test and the one-way ANOVA analyses of variance. The significance was set at $p < 0.05$. All data from statistical analyses presented in this thesis are expressed as a mean value with its standard deviation.

5. RESULTS AND DISCUSSION

5.1. MANUFACTURING AND TESTING OF INTERPENETRATED Mg/CaP SYSTEMS.

5.1.1 SYNTHESIS AND MANUFACTURING OF CaP SCAFFOLDS.

The syntheses of HA and β-TCP powders were performed through wet chemistry by the chemical precipitation method. The reaction was between phosphoric acid (H_3PO_4) and calcium hydroxide ($Ca(OH)_2$). For the consolidation of preforms made of HA and β-TCP, a sintering process can be carried out; this is not the case for CDHA-based structures because a thermal treatment decomposes this type of calcium phosphate. Thus, a solid-state reaction between monetite (calcium hydrogen phosphate, $CaHPO_4$) and calcium carbonate ($CaCO_3$) was carried out at a temperature of 1400 ºC in order to produce α-TCP powder, which was used for the robocasting of the preforms. Later, the α-TCP structures were hydrated to obtain consolidated CDHA preforms by inter-crossing a fine plate microstructure.

Figure 2 shows the XRD patterns from all the CaP powders used for the robocasting of porous preforms. Comparing the patterns with the standards and performing the Rietveld analysis:

- The initial HA powder was confirmed to be stoichiometric HA (ICSD: 087670).
- A minor trace of CDHA (0.5 wt.%) was detected in the β-TCP powder and the rest was pure rhombohedral TCP (β-TCP, ICSD: 006191).
- The initial α-TCP was single monoclinic TCP (α-TCP, ICSD: 000923).
- CDHA was formed by the hydrolysis of α-TCP; the composition analysis revealed the presence of two phases, mainly CDHA with 83.7 wt. % (ICSD: 087669) and unreacted monoclinic TCP (16.3 wt. %). The diffraction pattern indicated higher crystallinity for the α-TCP compared with the CDHA. This is judged from the shape of the diffraction peaks, which is connected to either non-crystalline microstructure or extremely small crystal size in the CDHA phase.

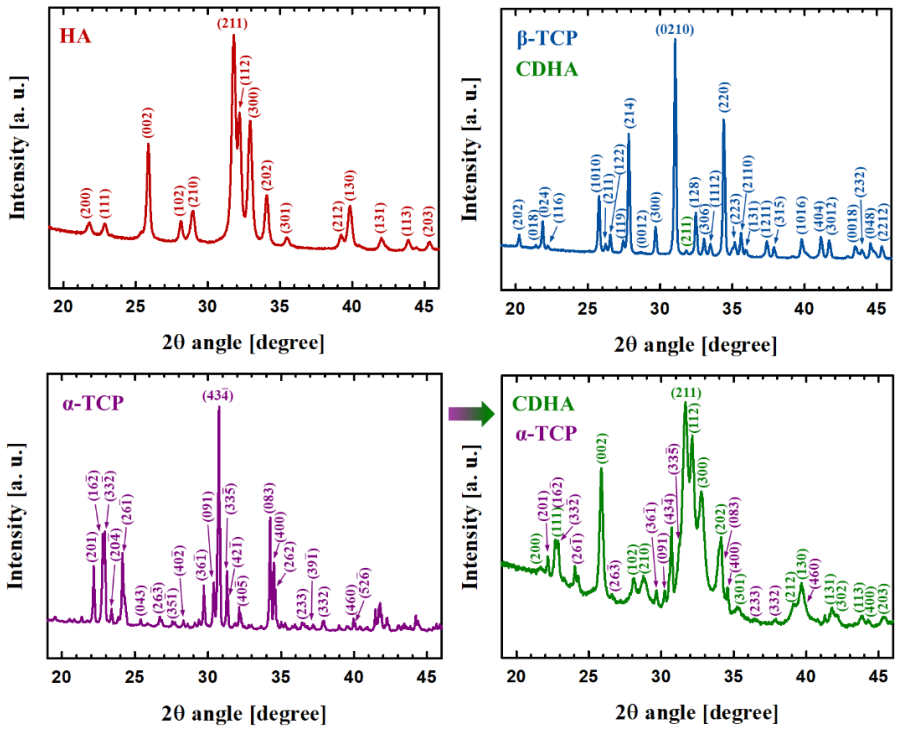

Figure 2. X-ray diffraction patterns of synthesised CaP powders. Arrow indicates the transformation of α-TCP after the hydrolysis.

The powders were used for the fabrication of porous cylinders following an orthogonal pattern with a designed pore size of 500 µm, which was changed after the consolidation of the structures, especially in the case of the structures that were sintered (HA and β-TCP).

5.1.2. CASTING OF PURE MG, MG-CA AND MG-ZN ALLOYS.

The used Mg alloys are listed in **Table 2** together with their elemental composition measured by X-ray fluorescence and atomic absorption spectroscopy for a precise estimation of calcium concentration.

Table 2. Elemental analysis (wt. %) of pure Mg and processed binary Mg alloys.

Nominal composition	Ca	Zn	Cu	Ni	Fe	Al	Si	Mn	Be
Pure Mg	0.0009	0.0028	0.0015	0.0015	0.0020	<0.01	0.012	0.034	0.00004
Mg-0.2%Ca	**0.26**	0.0032	0.0016	0.0011	0.0026	<0.01	0.028	0.033	0.00004
Mg-1%Zn	0.0008	**0.98**	0.0016	0.0017	0.0016	<0.01	0.012	0.035	0.00004

The X-ray diffraction patterns for the pure Mg and Mg alloys containing low amounts of Ca or Zn are shown in **Figure 3a**. The typical reflection peaks of the Mg alloys were the same as those for pure magnesium, revealing no formation of intermetallic phases. Characteristic microstructures of a pure Mg source and the cast Mg alloys are shown in **Figure 3**. The alloying elements together with the extrusion process led to a grain refinement effect of the alloys.

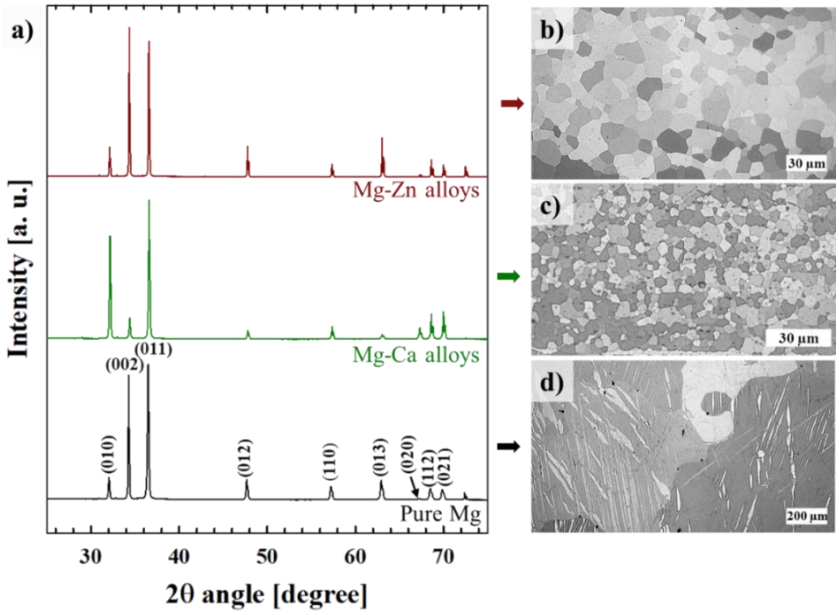

Figure 3. (a) Characteristic X-ray diffraction patterns of the initial pure Mg and Mg alloys. Representative optical micrographs of (b) Mg-1%Zn, (c) Mg-0.2%Ca, and (d) pure Mg.

5.2. CHARACTERIZATION OF INTERPENETRATED Mg/CaP COMPOSITES

After the infiltration, a visual examination on cut samples revealed a reaction between the ceramic phases and molten Mg. A change in the colour of the ceramic strands indicated that their interaction with Mg triggers the reduction reaction of the CaP preforms, forming MgO and decomposing the phosphate group. Previous investigations presumed the formation of gaseous phosphorous compounds such as phosphine (PH_3). For example, the reaction between pure Mg and β-TCP has been recorded between 520 ºC and 534 ºC as an exothermic phenomenon involving an abrupt mass loss due to the decomposition of the CaP ceramic [33]. After a visual examination, the TCP-based interpenetrated composites were discarded from further characterization due to the excess of decomposition of the ceramic phase. This effect was not

so evident for the composites formed with HA and CDHA preforms, which were the final interpenetrated Mg/CaP composites fully characterised in this study.

In order to evaluate the quality of the infiltration, random samples of the diverse Mg/CaP interpenetrated composites were taken for the µ-CT reconstruction. Representative images of the Mg/CaP composites from µ-CT are shown in **Figure 4**.

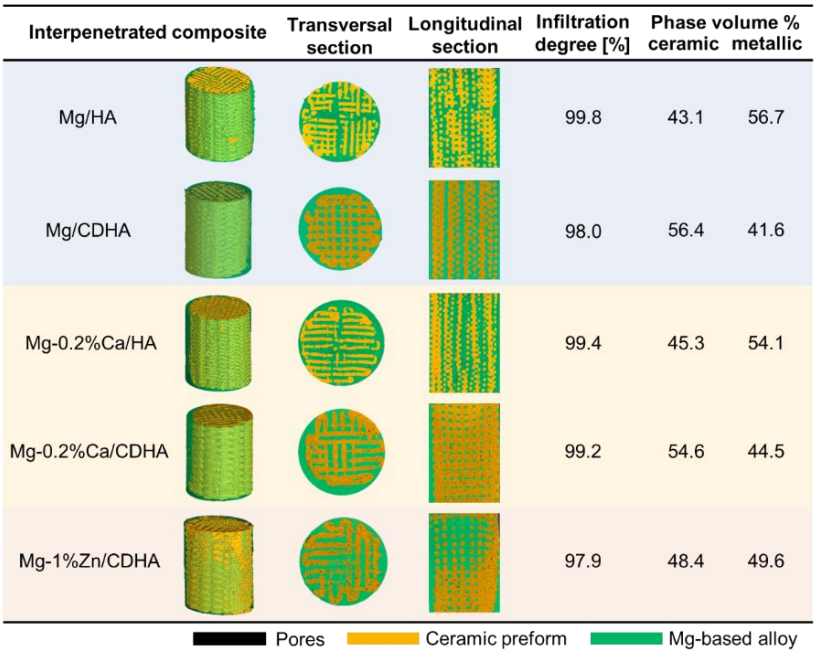

Figure 4. Image reconstruction made from X-ray computed tomography of Mg/CaP interpenetrated composites together with the calculated degree of infiltration and volumetric phase percent.

The infiltration produced an interface connection between the ceramic and the metallic phases. The interface is highlighted for the Mg/CDHA composite in **Figure 5a**; an SEM micrograph together with a lineal EDX analysis showed that the interface between the Mg and the CaPs consisted predominantly of Mg and O. Also, as a product of the chemical affinity between the CaP and molten Mg, the reduction of the CaP phase led to the dissolution of calcium ions into the Mg matrix, causing the precipitation of the eutectic Mg-Mg_2Ca phase (**Figure 5b-c**).

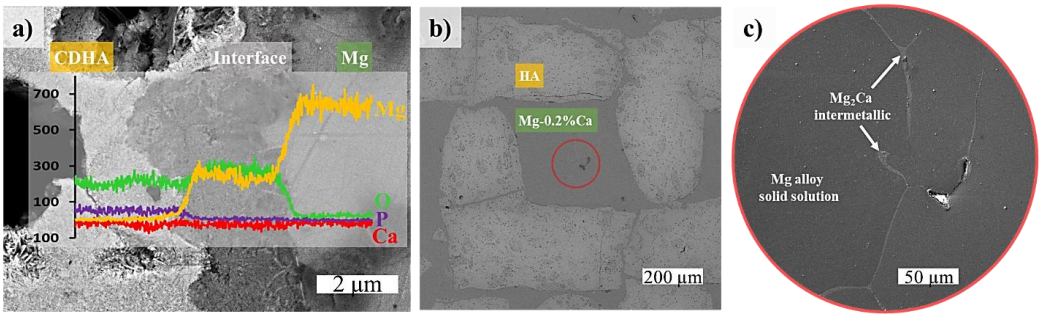

Figure 5. a) Lineal EDX analysis on typical interface between Mg and CaP. b) Representative micrograph of interpenetrated composites, Mg-0.2%Ca/HA with Mg_2Ca intermetallic phase; and c) detail of Mg phase pointing out the Mg_2Ca intermetallic as a product of the reduction of the CaP phase.

5.2.1. MECHANICAL BEHAVIOUR OF INTERPENETRATED MG/CAP COMPOSITES

A comparison of the mechanical behaviour of the Mg/CaP interpenetrated composites is summarized in **Table 3**.

Table 3. Compressive mechanical properties of interpenetrated Mg/CaP composites and the initial constituents.

Material	Yield strength [MPa]	Ultimate compression strength, σ_{max} [MPa]	Deformation [%]
HA preform	0.2±0.04	2.3±0.6	<0.2
CDHA preform	2.8±0.25	6.4±1.6	<0.8
Mg	154.3±31.2	172.9±23.8	27.1±4.7
Mg-0.2%Ca	164.8±6.4	358.5±2.4	19.5±0.1
Mg-1%Zn	103.6±2.8	336.1±7.4	17.7±0.3
Mg/HA	70.9±5.9	116.2±9.1	13.7±3.1
Mg-0.2%Ca/HA	60.8±8.6	119.2±32.7	14.8±1.6
Mg/CDHA	25.2±3.3	48.2±6.6	16.4±1.0
Mg-0.2%Ca/CDHA	23.9±1.8	40.9±5.1	13.9±1.5
Mg-1%Zn/CDHA	23.3±3.4	49.6±7.8	15.5±1.0

The initial porous preforms presented a very low mechanical strength, which is typical for porous ceramics [34]. CDHA preforms exhibited a better mechanical performance than the HA preforms did. Two main reasons can be taken into account as potential explanation: first, the difference in microstructure after the consolidation process, and second and most significant, the difference in the dimensions of strands that form the cylindrical preforms.

The mechanical behaviour was similar for all of the initial magnesium alloys. The Mg alloys had an average ultimate compressive strength of about 350 MPa, which was twice that of the pure Mg (~173 MPa). On the other hand, Mg-1%Zn alloy showed a rapid plastic deformation compared with the Mg-0.2%Ca alloy, which exhibited a larger region of elastic deformation. The different mechanical response of the Mg-based phases is attributed to the refining effect [35].

The interpenetrated Mg/CaP composites exhibited mechanical properties whose values were between those of their former constituents. This behaviour reflects the good connection between the phases. Despite the fact that the mechanical properties of the initial preforms showed contradictory behaviour, the composites constituted of HA preforms exhibited a higher strength than the CDHA-based composites did. The set of the HA-based interpenetrated composites were of analogous mechanical properties. The same behaviour was observed for the set of CDHA-based composites (**Figure 6**). This behaviour indicates that the mechanical properties of the interpenetrated composites are predominantly governed by the ceramic phase and they are not dependent on the Mg composition.

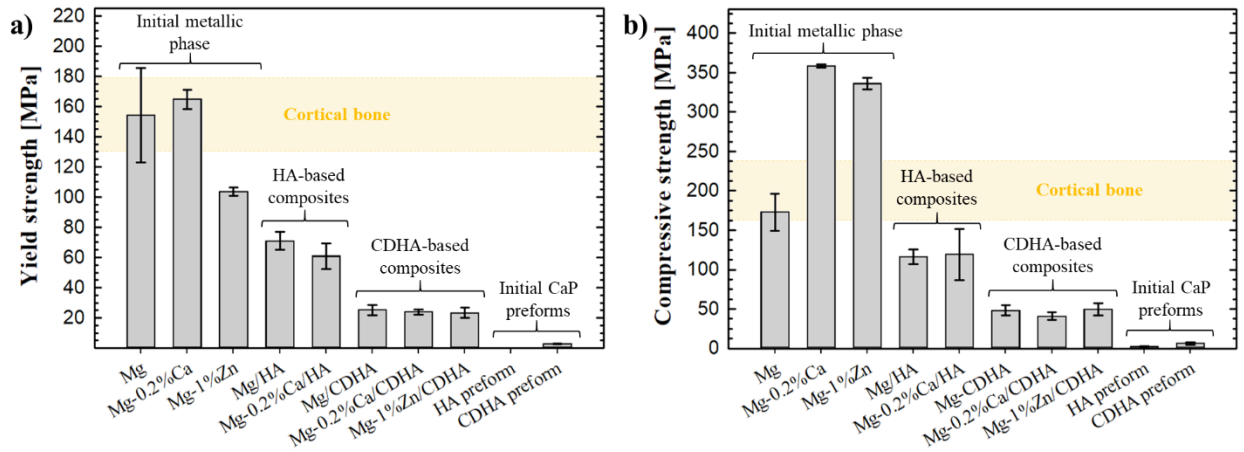

Figure 6. Room-temperature compressive mechanical properties of initial Mg alloys, CaP preforms, and processed interpenetrated composites: a) yield strength and b) ultimate compressive strength.

Despite the low strength of the Mg/CaP interpenetrated composites compared with the initial metallic phases, the infiltration of the ceramic scaffolds with Mg-based alloys provided a significant increase in the mechanical response of the infiltrated preforms and gave engineering strain to the composites. An inspection of the fracture surface of the Mg/CaP composites revealed that the failure mechanism relies on the chemical composition and/or morphology of the CaP preforms. For HA-based composites, the failure of the specimens occurred due to the cracking of the ceramic preform, whereas the CDHA-based composites failed predominantly by cleavage at the MgO interface between the ceramic preform and the metallic phase. This behaviour exposed the role of the interface thickness in the Mg/CaP composites; therefore, when the interface is large, the mechanical properties are compromised by the fragility of the MgO layer.

In general, the best-interpenetrated composites in terms of the mechanical properties were the Mg-0.2%Ca/HA, followed by the Mg/HA composite. These two interpenetrated composites exhibited an average deformation of ~14% and a compressive strength of ~120 MPa. These results are in agreement with other Mg/CaP composites manufactured by liquid infiltration [36–38].

Unfortunately, the mechanical properties of the interpenetrated Mg/CaP composites are below the prime requirements for cortical bone replacement. However, the ductility and compressive strength exhibited in these structured composites makes them still suitable in orthopaedic applications where the load does not exceed the mechanical limits of the specimens. Additionally, one of the main advantages of these Mg/CaP composites over the current materials for bone fixation, such as stainless steel, is not only the degradation but also the very low stress-shielding effect that this light composites can provide during bone healing.

Moreover, another advantage of the interpenetrated composites is that the mechanical response can be tailored by the geometrical distribution of the phases and/or by varying the metallic/ceramic phase ratio as it was observed between the Mg/HA and Mg/CDHA composites. This statement is one of the highlights of this type of composites presented here because in difference to other produced composites where the reinforcement phase is randomly distributed, in the architecture developed here, the phases are arranged in a predesigned pattern that can be modified to produce different distributions with diverse mechanical properties [39,40].

5.2.2. CORROSION RESISTANCE OF INTERPENETRATED MG/CAP COMPOSITES

In terms of corrosion resistance, the produced interpenetrated composites exhibited different behaviour. The measurements of the degradation rate were carried out primarily by H_2 evolution and potentiodynamic polarisation measurements. The selection of these two techniques was based on the fact that monitoring the produced hydrogen during the corrosion of Mg offers a reliable corrosion profile over a prolonged period of time. On the other hand, the electrochemical measurement provides knowledge of the initial corrosion mechanism and reaction kinetics for physiologically realistic media [41].

The corrosion rate of the different composite systems estimated by H_2 evolution during 14 days under physiological conditions (immersion in SBF at 37 ºC) are summarized in **Table 4**.

Table 4. Degradation rate of produced interpenetrated Mg/CaP composites and their metallic counterparts estimated by the H_2 evolution assessment after 2 weeks in SBF at 37 ºC.

Material	Corrosion rate [mm·year^{-1}]
Pure Mg	4.24 ± 0.29
Mg/HA	3.69 ± 1.67
Mg/CDHA	5.62 ± 3.80
Mg-0.2%Ca	2.88 ± 0.18
Mg-0.2%Ca/HA	11.12 ± 2.30
Mg-0.2%Ca/CDHA	4.87 ± 0.53
Mg-1%Zn	1.90 ± 0.66
Mg-1%Zn/CDHA	5.90 ± 2.59

In general, the interpenetrated composites had a faster corrosion rate than the Mg-1%Zn and Mg-0.2%Ca alloys, which were in the range of 2–3 mm·year^{-1}. Furthermore, the bare alloys presented almost twice the corrosion resistance of pure Mg, as expected from the difference in the grain size microstructure. The best interpenetrated composite in terms of its corrosion resistance was found in the Mg/HA material with an average corrosion rate of 3.69 mm·year^{-1} (estimated by H_2 evolution test). On the other hand, the fastest degradation rate was registered for the Mg-0.2%Ca/HA composite with a degradation rate of above 11 mm·year^{-1}.

The wide range of the corrosion profile is due to several factors: (1) the grain size of the metallic phase was increased during the non-controlled solidification during the CAMI process; (2) the effective surface area of the metallic phase in the interpenetrated composites varied from sample to sample; and (3) the porosity of the CaP ceramic phase and MgO interface could act as absorbent channels.

The assessment of the H_2 production also allowed recognizing the changes in the corrosion mechanism along the first two weeks under simulated physiological conditions. All the interpenetrated composites and initial Mg alloys reached a constant corrosion rate after the 5th day of immersion. This effect is common in Mg alloys due to the passivation of the surface by the formation of a protective $Mg(OH)_2$ layer and the deposition of calcium and phosphorus compounds [42].

Alternatively, the potentiodynamic polarisation test in SBF at room temperature revealed a similar tendency in the degradation rate of the composites to that in the initial profiles registered by H_2 evolution. In the case of pure Mg and its composites, the results revealed that the corrosion potential (E_{corr}) becomes

more negative in the following order: Mg/HA ≤ Mg/CDHA < pure Mg. By contrast, the Mg-0.2%Ca and Mg-1%Zn alloys revealed a less negative E_{corr} than their interpenetrated composites with HA and CDHA structures. The higher negative values in the E_{corr} of the composites compared to the Mg alloys is related to a faster corrosion rate. This effect is a consequence of the initial reactivity of the materials, which is increased by the grain size of the metallic phase and the presence of the Mg_2Ca intermetallic [43,44].

Table 5 summarizes the E_{corr}, corrosion current density (i_{corr}) and corrosion rate of the different systems calculated by Tafel extrapolation of the polarisation curves and Faraday's law.

Table 5. Corrosion potential, corrosion current density and degradation rate estimated by the Tafel extrapolation of obtained polarisation curves using SBF at room temperature.

Material	Corrosion potential, E_{corr} (V)	Corrosion current density, i_{corr} (mA·cm^{-2})	Corrosion rate [mm·year^{-1}]
Pure Mg	-1.89 ± 0.01	0.216 ± 0.00	4.93 ± 0.11
Mg/HA	-1.71 ± 0.05	0.408 ± 0.05	9.33 ± 1.17
Mg/CDHA	-1.78 ± 0.05	0.614 ± 0.15	12.68 ± 2.88
Mg-0.2%Ca	-1.66 ± 0.02	0.371 ± 0.12	8.49 ± 0.11
Mg-0.2%Ca/HA	-1.77 ± 0.07	0.533 ± 0.02	12.20 ± 0.52
Mg-0.2%Ca/CDHA	-1.78 ± 0.02	0.524 ± 0.07	12.00 ± 1.70
Mg-1%Zn	-1.65 ± 0.05	0.358 ± 0.03	8.17 ± 0.68
Mg-1%Zn/CDHA	-1.74 ± 0.01	0.473 ± 0.13	10.80 ± 3.09

The corrosion current density provides information about the cathodic reaction during the Mg corrosion, which is connected to the production of H_2 [45–47]. Lower values of i_{corr} indicate better corrosion resistance [37]. From this point of view, the pure metallic phases revealed lower corrosion current densities, consequently a higher corrosion resistance in comparison to the Mg/CaP interpenetrated composites. This can only be explained by the grain size of the magnesium phase and the presence of the Mg_2Ca intermetallic [43–45].

The corrosion rates estimated by the Tafel extrapolation measurements were almost three times higher than the values obtained by the H_2 evolution test after 14 days of immersion. This difference has been previously reported [41] and is predominantly influenced by two aspects: (1) the dissimilarity in the time of testing, i.e. 14 days vs. ~2 min; and (2) the difference in the exposed surface area to corrode. Despite the variance between the methods for the estimation of the corrosion rate in Mg and its alloys, the combination of them provides a better overview of the degradation resistance. In this sense, H_2 evolution divulges how much corrosion occurs in the course of time, while the potentiodynamic polarisation test reveals the mechanism involved in the corrosion process [44].

In general, all the produced materials exhibited pitting corrosion. Mg and its alloys usually become the anode when there are two components or when two different grain sizes exist within the same alloy [47]. In the case of the interpenetrated Mg/CaP composites, the pitting corrosion was rather a crevice corrosion, preferentially localised along the interface between the ceramic and metallic phases. This effect was previously observed for similar interpenetrated composites based on β-TCP+MgO/Zn-Mg and HA+ β-TCP/MgCa, where the process is explained because of the capability of the interface to create a galvanic couple with the ceramic phase [36,48].

To sum up, the produced Mg/CaP composites revealed a similar corrosion resistance and presented an equal corrosion mechanism. In general, the corrosion rate values of the interpenetrated Mg/CaP composites were slightly higher than the ones found in the literature for similar interpenetrated composites obtained by an infiltration of HA-TCP scaffolds with Mg-1%Ca alloy, with an average corrosion rate of about 3.4 mm·year^{-1} [17,37]. In spite of the fast corrosion rate in the interpenetrated Mg/CaP composites, they exhibited better corrosion resistance than the conventional composites based on Mg and Mg alloys with HA or β-TCP particles and produced by powder metallurgy or stirring casting (~1.5-720 mm·year^{-1}) [49,50].

5.2.3. CYTOTOXICITY AND CELL VIABILITY OF INTERPENETRATED MG/CAP COMPOSITES

The proliferation of SAOS-2 cells in extracts from Mg samples was evaluated by counting the number of cellular nuclei, using the image analysis of each well area after 1, 3 and 6 days of testing. **Figure 7** shows the proliferation of SAOS-2 cells from the indirect contact with the bare Mg, Mg alloys, and the interpenetrated Mg/CaP composites. The pure Mg revealed a constant number of cells over the time. The Mg-0.2%Ca alloy slightly promoted the cell proliferation after the 3rd day of cell culture while the Mg-1%Zn alloy did not reveal any significant difference in the cell proliferation over the testing time (**Figure 7a**).

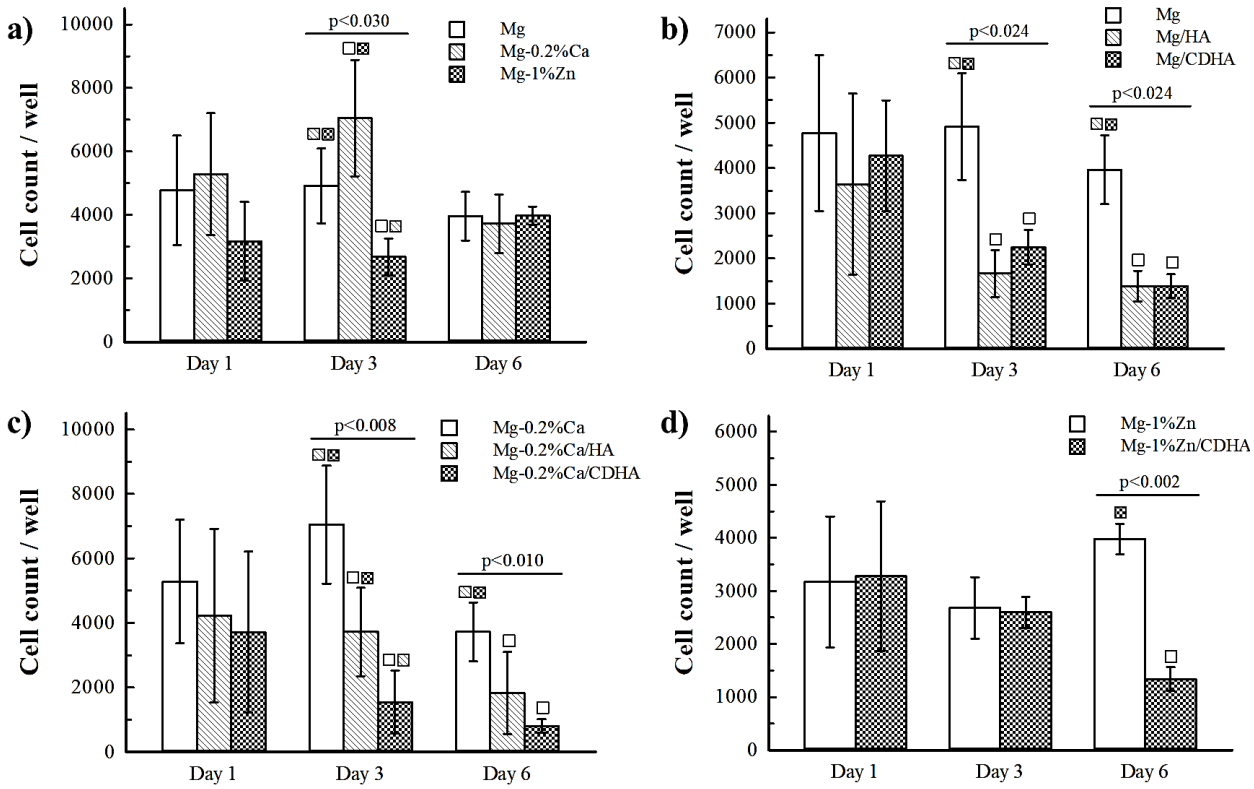

Figure 7. SAOS-2-cell proliferation represented as cell count per well. Data are expressed as the mean ± S.D. The significant differences between similar sets of samples at particular time points (Mann-Whitney U test; $p<0.05$; $n = 8$ per each group) are marked by corresponding group legend pattern.

In the case of the Mg-based composites, the Mg/HA and Mg/CDHA composites had a similar cell proliferation as the pure Mg phase after 24 hours of cell culture. However, the interpenetrated composites revealed a significant and equal decrease in the cell proliferation after the 3rd and 6th days (**Figure 7b**).

Similarly, the Mg-0.2%Ca/HA and Mg-0.2%Ca/CDHA composites revealed a decrease in the cell proliferation after the 3rd and 6th days of the test. Nevertheless, the Mg-0.2%Ca/HA composite exhibited a slightly better proliferation effect than the Mg-0.2%Ca/CDHA material over time (**Figure 7c**). The same behaviour was observed in the Mg-1%Zn/CDHA composite, where the proliferation of the SAOS-2 cells gradually decreased after the 3rd and 6th days of culture (**Figure 7d**).

The decrease in the proliferation is directly connected to the cytotoxic effect of the materials. Thus, the cytotoxicity of the Mg/CaP composites was estimated by means of the cellular viability of live SAOS-2 cells after their contact with the Mg/CaP composites for 1, 3 and 6 days (**Figure 8**). In general, all the Mg/CaP composites revealed higher cytotoxicity after the 3rd and 6th days of cell culture in comparison with the bare metallic phases (**Figure 8b-d**).

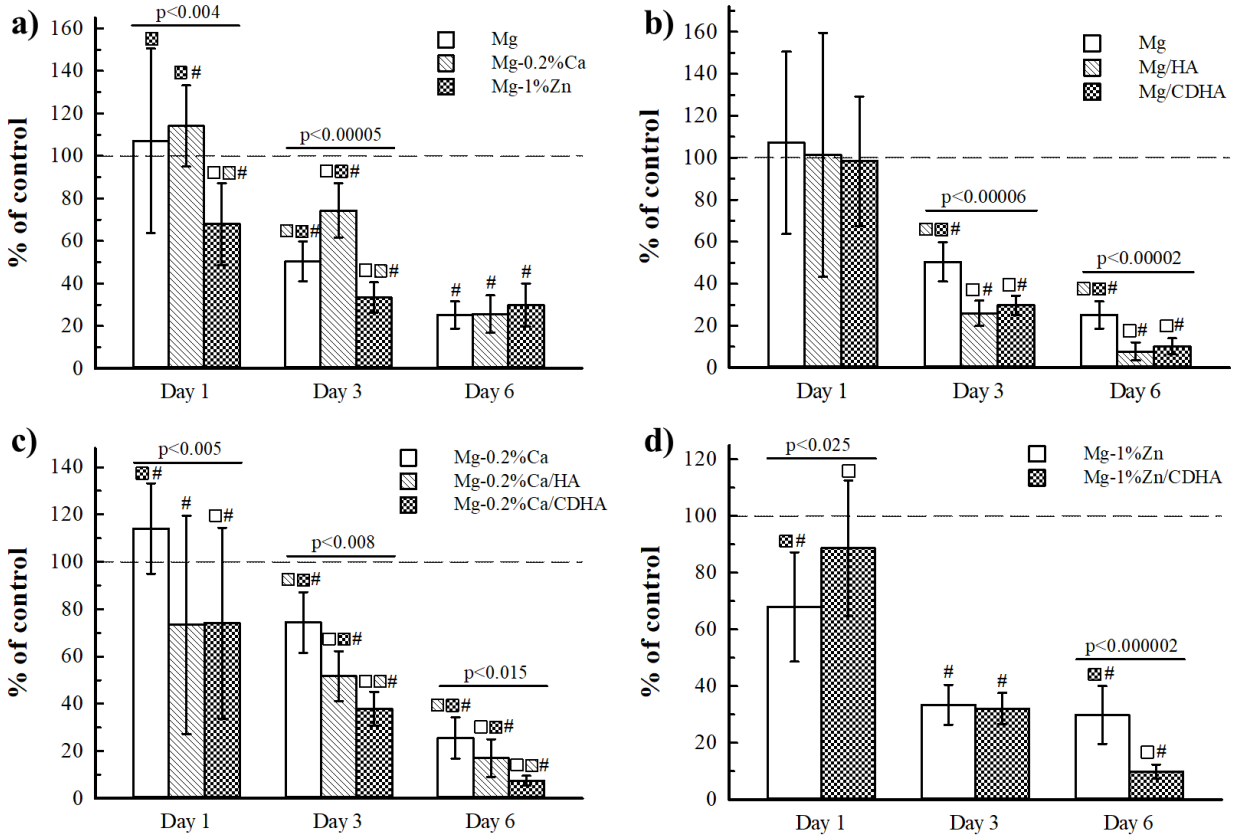

Figure 8. SAOS-2 viability represented as % of untreated control. Data are expressed as the mean ± S.D. The significant differences between similar sets of samples at particular time points (Mann-Whitney U test; $p<0.05$; n = 16 per each group) are marked by corresponding group legend pattern. The significant difference of a particular group from 100% of untreated control is marked by # (Student T-test, $p<0.05$; n = 16 per each group).

Interpenetrated MgCa/HA-TCP composites have revealed a cytotoxicity effect of grade II (mild cytotoxicity [51]) on the L-929 and MG-63 cells, with a constant cell viability of around 60 % during the first 5 days of culture [37]. This grade of cell viability is similar for the first 72 hours in the here studied

interpenetrated Mg/CaP composites. However, after the 6th day of cell culture, the interpenetrated composites revealed a significant decrease in cell viability reporting values below the 30 %, which denotes grade III in cytotoxicity (moderate reactivity of the material on the SAOS-2 cells), ISO 10993-5:2009. This cytotoxic effect is explained by the synergetic effect of high osmolarity and pH that exposes the investigated cells to an osmotic shock. From this point of view, nearly all Mg-alloy-based materials would be classified as cytotoxic, as the corrosion of Mg increases the pH between ~9.0-11.5, and at the same time that alters the ion concentration of the *in vitro* media [19,37,45].

The high reactivity of the Mg-based composites makes difficult the *in-vitro* test procedures, which, in addition, do not correlate well with the *in-vivo* data [52]. In view of the above, the indirect *in-vitro* test can be improved by the use of diluted extracts obtained from the corrosion of the tested Mg-based materials. For instance, 50% and 10% degrees of extract dilution significantly improved the cell viability values of interpenetrated MgCa/HA-TCP composites (up to grade I, slight cytotoxicity) by lowering the effect of a high pH [37]. The same positive results have been reported for the Mg-Zn/β-TCP composites, which exhibited a cytotoxicity below grade I in L-929 cells cultured in similar diluted extracts of the corrosion products. Moreover, this testing methodology agreed better with the good biocompatibility obtained *in vivo* for bone tissue of rabbits [53]. Consequently, despite the low cell viability revealed by the interpenetrated Mg/CaP composites, *in vivo* studies have shown the great potential of Mg-based biomaterials, as is the case of pure Mg and alloys such as AZ91D, LAE442, Mg-Li-Ca, and MgCaP composites [31,54,55].

To sum up, the ineffective biocompatibility of the manufactured Mg/CaP was mainly connected to the fast degradation behaviour, which was accompanied by the pH increasing up to an average value of 9.5. Still, based on previous results for similar Mg/CaP composites, these types of materials can find a potential application as degradable biomaterials for orthopaedics [37,53,56]. The main issues to be solved with this aim are the control of the microstructure and also the degradation behaviour, which will enhance the biocompatibility response in the cells that would be in contact with the materials.

6. CONCLUSIONS

The existing considerable knowledge of biomaterials for orthopaedics is being continuously developed. Nevertheless, the necessity of innovating temporal bone-regeneration implants that allow the healing of defective bone tissue and degrade after accomplishing their function must go hand in hand with satisfying the patients and granting them the best possible treatment. In the thesis, a detailed study on the processing of Mg alloys together with calcium phosphates has been performed with the aim to evaluate the feasibility of their composites as temporary bone-healing implants. The design of the Mg/CaP composites was established in an original way, combining additive manufacturing (robocasting) with a newly introduced metal infiltration technique in order to produce interconnected architectural composite structures.

Porous structures with controlled pore size and designed architectural geometry were successfully produced by depositing ceramic pastes, following an orthogonal pattern, to build up cylindrical scaffolds consisting of stoichiometric HA, α-TCP and β-TCP ceramic phase.

The CAMI was introduced for the first time and proved to be a novel technique for the infiltration of ceramic preforms with a molten metal such as Mg and Mg alloys. The CAMI process allows the manufacturing of interconnected composites with different melting points in only a few minutes and under

controlled atmosphere. The combination of the CAMI process with additive manufacturing techniques allows the production of innovative interconnected composites with a diverse organized distribution of the phases according to the requirements of the final application.

The study proved that the infiltration success was above 98 % of the initial porosity of the scaffolds. This was achieved not only due to the infiltration technique but also because of the chemical affinity between the materials used. Significant differences between Mg/HA and Mg/CDHA interconnected composites were found based on the chemical composition, phase distribution and chemical affinity between the constituents of the composites. By way of microstructural characterization the higher reactivity between Mg and its alloys with CDHA was observed, resulting in a thicker MgO interface formation compared with the stoichiometric HA composites. The dissolution of the CaP preforms led to the precipitation of the Mg_2Ca intermetallic phase, which is unfavourable for the mechanical and corrosion resistance properties because of its brittleness and formation of a galvanic couple with the pure Mg or Mg alloy matrix during the corrosion process.

The resulting microstructure of the metallic phase after the infiltration process consisted of large crystal grains. This coarse microstructure detrimentally affected not only the mechanical properties but also the corrosion behaviour.

In terms of mechanical properties, the manufactured Mg/CaP composites exhibited the required mechanical response under compression for its function as substitutes of cancellous and low-load-bearing cortical bone according to their compressive strength and excellent failure strain above 10 % of deformation before its mechanical failure. In general, HA-based composites revealed better performance, exhibiting almost twice the compressive strength of the CDHA-based composites; which is attributed to: (1) the higher amount of ceramic phase due to its shrinkage after consolidation; and (2) the thicker MgO interface that forms in a cleavage fracture.

In general, the Mg/CaP composites exhibited a faster corrosion rate than the pure Mg phases did. The HA-based composites revealed better corrosion resistance compared with their CDHA counterparts. This was attributed to the microstructure of the ceramic preforms, which in the case of the CDHA acted as an absorbent of liquid solution (SBF), promoting the corrosion of the metallic phase even in the inner part of the bulk composite body.

As a product of the fast corrosion, the cytocompatibility evaluation resulted in a low affinity of the material with SAOS-2 cells due to the increase in the pH. In the proliferation test, the bare metals revealed a better cytocompatibility response than their composites along the first week of testing.

Finally, despite the cytotoxic response of the interpenetrated Mg/CaP composites, the development of these types of materials can still have a potential for their application as degradable biomaterials. This is based on the assumption that the cytocompatibility response can be enhanced by controlling the microstructure and degradation of the Mg-based phase, maintaining a suitable mechanical performance for the production of temporal orthopaedic devices.

BIBLIOGRAPHY

[1] A. Svedbom, E. Hernlund, M. Ivergård, J. Compston, C. Cooper, J. Stenmark, E. V. McCloskey, B. Jönsson, J.A. Kanis, Osteoporosis in the European Union: a compendium of country-specific reports, *Arch. Osteoporos.* 8 (**2013**) 137. https://doi.org/10.1007/s11657-013-0137-0.

[2] A.K. Nasution, H. Hermawan, Degradable Biomaterials for Temporary Medical Implants BT - Biomaterials and Medical Devices: A Perspective from an Emerging Country, in: F. Mahyudin, H. Hermawan (Eds.), Springer International Publishing, Cham, **2016**: pp. 127–160. https://doi.org/10.1007/978-3-319-14845-8_6.

[3] F. Witte, F. Feyerabend, P. Maier, J. Fischer, M. Störmer, C. Blawert, W. Dietzel, N. Hort, Biodegradable magnesium–hydroxyapatite metal matrix composites, *Biomaterials*. 28 (**2007**) 2163–2174. https://doi.org/10.1016/j.biomaterials.2006.12.027.

[4] R.Z. LeGeros, J.P. LeGeros, Calcium phosphate Bioceramics: Past, present and future, *Bioceram. 15*. 240–2 (**2003**) 3–10. https://doi.org/DOI 10.4028/www.scientific.net/kem.240-242.3.

[5] F. Witte, The history of biodegradable magnesium implants: A review, *Acta Biomater.* 6 (**2010**) 1680–1692. https://doi.org/10.1016/j.actbio.2010.02.028.

[6] A.K. Khanra, H.C. Jung, K.S. Hong, K.S. Shin, Comparative property study on extruded Mg-HAP and ZM61-HAP composites, *Mater. Sci. Eng. A*. 527 (**2010**) 6283–6288. https://doi.org/10.1016/j.msea.2010.06.031.

[7] K. Mensah-Darkwa, R.K. Gupta, D. Kumar, Mechanical and Corrosion Properties of Magnesium–Hydroxyapatite (Mg–HA) Composite Thin Films, *J. Mater. Sci. Technol.* 29 (**2013**) 788–794. https://doi.org/10.1016/j.jmst.2013.04.019.

[8] S. Grasso, Y. Sakka, G. Maizza, Electric current activated/assisted sintering (ECAS): a review of patents 1906–2008, *Sci. Technol. Adv. Mater.* 10 (**2009**) 053001. https://doi.org/10.1088/1468-6996/10/5/053001.

[9] M. Prakasam, J. Locs, K. Salma-Ancane, D. Loca, A. Largeteau, L. Berzina-Cimdina, Biodegradable Materials and Metallic Implants—A Review, *J. Funct. Biomater.* 8 (**2017**) 44. https://doi.org/10.3390/jfb8040044.

[10] A.R. Amini, J.S. Wallace, S.P. Nukavarapu, Short-term and long-term effects of orthopedic biodegradable implants, *J. Long. Term. Eff. Med. Implants*. 21 (**2011**) 93–122. https://doi.org/10.1615/jlongtermeffmedimplants.v21.i2.10.

[11] H. YUAN, Z. YANG, Y. LI, X. ZHANG, J.D. DE BRUIJN, K. DE GROOT, Osteoinduction by calcium phosphate biomaterials, *J. Mater. Sci. Mater. Med.* 9 (**1998**) 723–726. https://doi.org/10.1023/a:1008950902047.

[12] B.S. Chang, C.K. Lee, K.S. Hong, H.J. Youn, H.S. Ryu, S.S. Chung, K.W. Park, Osteoconduction at porous hydroxyapatite with various pore configurations, *Biomaterials*. 21 (**2000**) 1291–1298. https://doi.org/10.1016/s0142-9612(00)00030-2.

[13] B. Bourgeois, O. Laboux, L. Obadia, O. Gauthier, E. Betti, E. Aguado, G. Daculsi, J.-M. Bouler, Calcium-deficient apatite: A firstin vivo study concerning bone ingrowth, *J. Biomed. Mater. Res.* 65A (**2003**) 402–408. https://doi.org/10.1002/jbm.a.10518.

[14] R.G. Carrodeguas, S. De Aza, α-Tricalcium phosphate: Synthesis, properties and biomedical applications, *Acta Biomater.* 7 (**2011**) 3536–3546. https://doi.org/10.1016/j.actbio.2011.06.019.

[15] L. Wang, G.H. Nancollas, Calcium Orthophosphates: Crystallization and Dissolution, *Chem. Rev*. 108 (**2008**) 4628–4669. https://doi.org/10.1021/cr0782574.

[16] M.P. Staiger, A.M. Pietak, J. Huadmai, G. Dias, Magnesium and its alloys as orthopedic biomaterials: A review, *Biomaterials*. 27 (**2006**) 1728–1734. https://doi.org/10.1016/j.biomaterials.2005.10.003.

[17] N. Li, Y. Zheng, Novel Magnesium Alloys Developed for Biomedical Application: A Review, *J. Mater. Sci. Technol.* 29 (**2013**) 489–502. https://doi.org/10.1016/j.jmst.2013.02.005.

[18] Y. Chen, Z. Xu, C. Smith, J. Sankar, Recent advances on the development of magnesium alloys for biodegradable implants, *Acta Biomater.* 10 (**2014**) 4561–4573. https://doi.org/10.1016/j.actbio.2014.07.005.

[19] F. Witte, N. Hort, C. Vogt, S. Cohen, K.U. Kainer, R. Willumeit, F. Feyerabend, Degradable biomaterials based on magnesium corrosion, *Curr. Opin. Solid State Mater. Sci.* 12 (**2008**) 63–72. https://doi.org/10.1016/j.cossms.2009.04.001.

[20] Y.F. Zheng, X.N. Gu, F. Witte, Biodegradable metals, *Mater. Sci. Eng. R Reports*. 77 (**2014**) 1–34. https://doi.org/10.1016/j.mser.2014.01.001.

[21] I.I.I. Cesarano Joseph (Albuquerque, NM), P.D. (Tucson Calvert AZ), Freeforming objects with low-binder slurry, **2000**. https://www.osti.gov/servlets/purl/872863.

[22] J.A. Lewis, J.E. Smay, J. Stuecker, J. Cesarano, Direct ink writing of three-dimensional ceramic structures, *J. Am. Ceram. Soc.* 89 (**2006**) 3599–3609. https://doi.org/10.1111/j.1551-2916.2006.01382.x.

[23] J. Franco, P. Hunger, M.E. Launey, A.P. Tomsia, E. Saiz, Direct write assembly of calcium phosphate scaffolds using a water-based hydrogel, *Acta Biomater.* 6 (**2010**) 218–228.

[24] P. Miranda, A. Pajares, E. Saiz, A.P. Tomsia, F. Guiberteau, Mechanical properties of calcium phosphate scaffolds fabricated by robocasting, *J. Biomed. Mater. Res. Part A.* 85A (**2008**) 218–227. https://doi.org/10.1002/jbm.a.31587.

[25] A. Mattern, B. Huchler, D. Staudenecker, R. Oberacker, A. Nagel, M.J. Hoffmann, Preparation of interpenetrating ceramic–metal composites, *J. Eur. Ceram. Soc.* 24 (**2004**) 3399–3408. https://doi.org/10.1016/j.jeurceramsoc.2003.10.030.

[26] K.M. Sree Manu, L. Ajay Raag, T.P.D. Rajan, M. Gupta, B.C. Pai, Liquid Metal Infiltration Processing of Metallic Composites: A Critical Review, *Metall. Mater. Trans. B.* 47 (**2016**) 2799–2819. https://doi.org/10.1007/s11663-016-0751-5.

[27] L. Hu, A. Kothalkar, M. O'Neil, I. Karaman, M. Radovic, Current-Activated, Pressure-Assisted Infiltration: A Novel, Versatile Route for Producing Interpenetrating Ceramic–Metal Composites, *Mater. Res. Lett.* 2 (**2014**) 124–130. https://doi.org/10.1080/21663831.2013.873498.

[28] S.D. de la Torre, L. Čelko, M.C. Luna, E.B.M. Jiménez, On the preparation of advanced materials via pulsed electric current sintering procedures, in: Solid State Phenom., **2017**: pp. 436–439. https://doi.org/10.4028/www.scientific.net/ssp.258.436.

[29] M. Casas-Luna, S. Tkachenko, M. Horynová, L. Klakurková, P. Gejdos, S. Diaz-De-La-Torre, L. Celko, J. Kaiser, E.B. Montufar, Interpenetrated magnesium-tricalcium phosphate composite: Manufacture, characterization and in vitro degradation test, *Acta Metall. Sin. (English Lett.* 30 (**2017**). https://doi.org/10.1007/s40195-017-0560-0.

[30] N. Sezer, Z. Evis, S.M. Kayhan, A. Tahmasebifar, M. Koç, Review of magnesium-based biomaterials and their applications, *J. Magnes. Alloy.* 6 (**2018**) 23–43. https://doi.org/10.1016/j.jma.2018.02.003.

[31] K. Kuśnierczyk, M. Basista, Recent advances in research on magnesium alloys and magnesium–calcium phosphate composites as biodegradable implant materials, *J. Biomater. Appl.* 31 (**2017**) 878–900. https://doi.org/10.1177/0885328216657271.

[32] M. Tamai, M. Nakamura, T. Isshiki, K. Nishio, H. Endoh, A. Nakahira, A metastable phase in thermal decomposition of Ca-deficient hydroxyapatite, *J. Mater. Sci. Mater. Med.* 14 (**2003**) 617–622. https://doi.org/10.1023/a:1024075008165.

[33] K. Narita, E. Kobayashi, T. Sato, Sintering Behavior and Mechanical Properties of Magnesium/β-Tricalcium Phosphate Composites Sintered by Spark Plasma Sintering, *Mater. Trans.* 57 (**2016**) 1620–1627. https://doi.org/10.2320/matertrans.l-m2016827.

[34] H. Zhao, L. Li, S. Ding, C. Liu, J. Ai, Effect of porous structure and pore size on mechanical strength of 3D-printed comby scaffolds, *Mater. Lett.* 223 (**2018**) 21–24. https://doi.org/10.1016/j.matlet.2018.03.205.

[35] Y. Uematsu, K. Tokaji, M. Kamakura, K. Uchida, H. Shibata, N. Bekku, Effect of extrusion conditions on grain refinement and fatigue behaviour in magnesium alloys, *Mater. Sci. Eng. A.* 434 (**2006**) 131–140. https://doi.org/10.1016/j.msea.2006.06.117.

[36] X.L. Ma, L.H. Dong, X. Wang, Microstructure, mechanical property and corrosion behavior of co-continuous β-TCP/MgCa composite manufactured by suction casting, *Mater. Des.* 56 (**2014**) 305–312. https://doi.org/10.1016/j.matdes.2013.11.041.

[37] X.N. Gu, X. Wang, N. Li, L. Li, Y.F. Zheng, X. Miao, Microstructure and characteristics of the metal-ceramic composite (MgCa-HA/TCP) fabricated by liquid metal infiltration, *J. Biomed. Mater. Res. Part B Appl. Biomater.* 99B (**2011**) 127–134. https://doi.org/10.1002/jbm.b.31879.

[38] X. Wang, J.T. Li, M.Y. Xie, L.J. Qu, P. Zhang, X.L. Li, Structure, mechanical property and corrosion behaviors of (HA + β-TCP)/Mg–5Sn composite with interpenetrating networks, *Mater. Sci. Eng. C.* 56 (**2015**) 386–392. https://doi.org/10.1016/j.msec.2015.06.047.

[39] H.F. Lei, Z.Q. Zhang, B. Liu, Effect of fiber arrangement on mechanical properties of short fiber reinforced

composites, *Compos. Sci. Technol.* 72 (**2012**) 506–514. https://doi.org/10.1016/j.compscitech.2011.12.011.

[40] A. Kaķitis, I. Nulle, D. Ancans, Mechanical properties of composite biomass briquettes, in: Vide. Tehnol. Resur. - Environ. Technol. Resour., Rezekne Higher Education Institution, **2011**: pp. 175–182. https://doi.org/10.17770/etr2011vol1.898.

[41] G. Song, A. Atrens, D. StJohn, An Hydrogen Evolution Method for the Estimation of the Corrosion Rate of Magnesium Alloys, in: Essent. Readings Magnes. Technol., Springer International Publishing, Cham, **2016**: pp. 565–572. https://doi.org/10.1007/978-3-319-48099-2_90.

[42] M. Esmaily, J.E. Svensson, S. Fajardo, N. Birbilis, G.S. Frankel, S. Virtanen, R. Arrabal, S. Thomas, L.G. Johansson, Fundamentals and advances in magnesium alloy corrosion, *Prog. Mater. Sci.* 89 (**2017**) 92–193. https://doi.org/10.1016/j.pmatsci.2017.04.011.

[43] G. Song, D. StJohn, The effect of zirconium grain refinement on the corrosion behaviour of magnesium-rare earth alloy MEZ, *J. Light Met.* 2 (**2002**) 1–16. https://doi.org/10.1016/s1471-5317(02)00008-1.

[44] N.T. Kirkland, N. Birbilis, M.P. Staiger, Assessing the corrosion of biodegradable magnesium implants: A critical review of current methodologies and their limitations, *Acta Biomater.* 8 (**2012**) 925–936. https://doi.org/10.1016/j.actbio.2011.11.014.

[45] H.R.B. Rad, M.H. Idris, M.R.A. Kadir, S. Farahany, Microstructure analysis and corrosion behavior of biodegradable Mg–Ca implant alloys, *Mater. Des.* 33 (**2012**) 88–97. https://doi.org/10.1016/j.matdes.2011.06.057.

[46] G. Song, A. Atrens, Understanding Magnesium Corrosion—A Framework for Improved Alloy Performance, *Adv. Eng. Mater.* 5 (**2003**) 837–858. https://doi.org/10.1002/adem.200310405.

[47] R.-C. Zeng, Z.-Z. Yin, X.-B. Chen, D.-K. Xu, Corrosion Types of Magnesium Alloys, in: Magnes. Alloy. - Sel. Issue, IntechOpen, **2018**. https://doi.org/10.5772/intechopen.80083.

[48] X. Wang, L.H. Dong, J.T. Li, X.L. Li, X.L. Ma, Y.F. Zheng, Microstructure, mechanical property and corrosion behavior of interpenetrating (HA+β-TCP)/MgCa composite fabricated by suction casting, *Mater. Sci. Eng. C.* 33 (**2013**) 4266–4273. https://doi.org/10.1016/j.msec.2013.06.018.

[49] R. Radha, D. Sreekanth, Mechanical and corrosion behaviour of hydroxyapatite reinforced Mg-Sn alloy composite by squeeze casting for biomedical applications, *J. Magnes. Alloy.* (**2019**). https://doi.org/10.1016/j.jma.2019.05.010.

[50] R. del Campo, B. Savoini, A. Muñoz, M.A. Monge, G. Garcés, Mechanical properties and corrosion behavior of Mg–HAP composites, *J. Mech. Behav. Biomed. Mater.* 39 (**2014**) 238–246. https://doi.org/10.1016/j.jmbbm.2014.07.014.

[51] M. Assad, N. Jackson, Biocompatibility Evaluation of Orthopedic Biomaterials and Medical Devices: A Review of Safety and Efficacy Models, in: Encycl. Biomed. Eng., Elsevier, **2019**: pp. 281–309. https://doi.org/10.1016/b978-0-12-801238-3.11104-3.

[52] J. Fischer, M.H. Prosenc, M. Wolff, N. Hort, R. Willumeit, F. Feyerabend, Interference of magnesium corrosion with tetrazolium-based cytotoxicity assays☆, *Acta Biomater.* 6 (**2010**) 1813–1823. https://doi.org/10.1016/j.actbio.2009.10.020.

[53] K. Yu, L. Chen, J. Zhao, S. Li, Y. Dai, Q. Huang, Z. Yu, In vitro corrosion behavior and in vivo biodegradation of biomedical β-Ca3(PO4)2/Mg–Zn composites, *Acta Biomater.* 8 (**2012**) 2845–2855. https://doi.org/10.1016/j.actbio.2012.04.009.

[54] F. Witte, J. Fischer, J. Nellesen, H.-A. Crostack, V. Kaese, A. Pisch, F. Beckmann, H. Windhagen, In vitro and in vivo corrosion measurements of magnesium alloys, *Biomaterials.* 27 (**2006**) 1013–1018. https://doi.org/10.1016/j.biomaterials.2005.07.037.

[55] D. Xia, Y. Liu, S. Wang, R.-C. Zeng, Y. Liu, Y. Zheng, Y. Zhou, In vitro and in vivo investigation on biodegradable Mg-Li-Ca alloys for bone implant application, *Sci. China Mater.* 62 (**2019**) 256–272. https://doi.org/10.1007/s40843-018-9293-8.

[56] P. Guo, Z. Cui, L. Yang, L. Cheng, W. Wang, B. Xu, Preparation of Mg/Nano-HA Composites by Spark Plasma Sintering Method and Evaluation of Different Milling Time Effects on Their Microhardness, Corrosion Resistance, and Biocompatibility, *Adv. Eng. Mater.* 19 (**2017**) 1600294. https://doi.org/10.1002/adem.201600294.

SUMMARY OF AUTHOR'S ACTIVITIES:

LIST OF PUBLICATIONS

[1] E.B. Montufar, K. Slámečka, **M. Casas-Luna**, P. Skalka, E. Ramírez-Cedillo, M. Zbončák, J. Kaiser, L. Čelko, Factors governing the dimensional accuracy and fracture modes under compression of regular and shifted orthogonal scaffolds, J. Eur. Ceram. Soc. (**2020**). //doi.org/10.1016/j.jeurceramsoc.2020.03.045

[2] **M. Casas-Luna**, J.A. Torres-Rodríguez, O.U. Valdés-Martínez, N. Obradović, K. Slámečka, K. Maca, J. Kaiser, E.B. Montúfar, L. Čelko, Robocasting of controlled porous CaSiO3–SiO2 structures: Architecture – Strength relationship and material catalytic behavior, Ceram. Inter.46 (**2020**) 8853-8861. https://doi.org/10.1016/j.ceramint.2019.12.130

[3] L. Čelko, M. Menelaou, **M. Casas-Luna**, M. Horynová, T. Musálek, M. Remešová, S. Diaz-De-La-Torre, K. Morsi, J. Kaiser, Spark Plasma Extrusion and the Thermal Barrier Concept, Metall. Mater. Trans. B 50 (**2019**) 656-665. https://doi.org/10.1007/s11663-018-1493-3

[4] **M. Casas-Luna**, H. Tan, S. Tkachenko, D. Salamon, E.B. Montufar, Enhancement of mechanical properties of 3D-plotted tricalcium phosphate scaffolds by rapid sintering, J. Eur. Ceram. Soc. 39 (**2019**) 4366-4374. https://doi.org/10.1016/j.jeurceramsoc.2019.05.055

[5] S. Tkachenko, M. Horynová, **M. Casas-Luna**, S. Diaz-de-la-Torre, K. Dvořák, L. Celko, J. Kaiser, E.B. Montufar, Strength and fracture mechanism of iron reinforced tricalcium phosphate cermet fabricated by spark plasma sintering. J. Mech. Biomed. Mater. 81 (**2018**) 16-25. //doi.org/10.1016/j.jmbbm.2018.02.016

[6] E.B. Montufar, **M. Casas-Luna**, M. Horynová, S. Tkachenko, Z. Fohlerová, S. Diaz-de-la-Torre, K. Dvořák, L. Čelko, J. Kaiser, High strength, biodegradable and cytocompatible alpha tricalcium phosphate-iron composites for temporal reduction of bone fractures. Acta Biomater. 70 (**2018**) 293-303. https://doi.org/10.1016/j.actbio.2018.02.002

[7] **M. Casas-Luna**, M. Horynová, S. Tkachenko, L. Klakurková, L. Celko, S. Diaz-de-la-Torre, E. Montufar, Chemical Stability of Tricalcium Phosphate–Iron Composite during Spark Plasma Sintering. J. Comp. Sci. 2 (**2018**) 51. https://doi.org/10.3390/jcs2030051

[8] **M. Casas-Luna**, S. Tkachenko, M. Horynová, L. Klakurková, P. Gejdos, S. Diaz-De-La-Torre, L. Celko, J. Kaiser, E.B. Montufar, Interpenetrated magnesium–tricalcium phosphate composite: Manufacture, characterization and in vitro degradation test. Acta Metall. Sinica (English Letters) 30 (**2017**) 319-325. https://doi.org/10.1007/s40195-017-0560-0

[9] E.B. Montufar, M. Horynová, **M. Casas-Luna**, S. Diaz-De-La-Torre, L. Celko, L. Klakurková, Z. Spotz, G. Diéguez-Trejo, Z. Fohlerová, K. Dvorak, Spark Plasma Sintering of Load-Bearing Iron–Carbon Nanotube-Tricalcium Phosphate CerMets for Orthopaedic Applications. JOM 68 (**2016**) 1134-1142. https://doi.org/10.1007/s11837-015-1806-9

PATENTS

- Mexican patent No. 365570: "Proceso de obtención de compósitos metálicos porosos con hidroxiapatita para implantes y el compósito de metal-hidroxiapatita" (Fabrication process of porous metallic composites with hydroxyapatite for implants and the metal-hydroxyapatite composite).
- Patent application MX/a/2015/016632: "Proceso de infiltración metálica en redes porosas cerámicas y/o metálicas utilizando la técnica de sinterizado por infiltración asistida por corriente eléctrica" (Metal infiltration process of porous ceramics and/or metallic networks using the technique of current-assisted infiltration sintering).

INTERNSHIP, TRAININGS AND OTHER ACTIVITIES

Internships:

- 2-month training internship (summer 2017) at the Magnesium Innovation Centre in the Helmholtz Centre in Geesthacht, Germany (MAGIC – HZG), under the supervision of Prof. Norbert Hort. The internship helped me in the design and casting of magnesium alloys containing calcium and zinc.
- 2-month internship (spring 2018) at the National Polytechnic Institute of Mexico (CIITEC – IPN) with Prof. Sebastián Díaz de la Torre, in order to perform the infiltration of calcium phosphate scaffolds with magnesium and Mg alloys

Trainings:

- Self-user of the core facilities at CEITEC-VUT for SEM-EDX, XRD, XPS, RAMAN, micro hardness indentation, metallographic preparation

Conferences:

- 8th International Conference on Materials Structure & Micromechanics of Fracture (MSMF8).
- 2015 and 2017 European Biomaterial Society Congress
- OZ-16 International Symposium on Nanostructures
- 25th ISMANAM congress
- 10th BIOMETAL congress
- Advanced Ceramics Applications VII 2018 congress
- Advanced Ceramics Applications VIII 2019 congress
- Fracture of Advanced Ceramics 2019 congress

Awards and scholarships:

- PhD Talent 2015
- Erasmus-trainings
- CEITEC PhD scholarship

PARTICIPATION IN RESEARCH PROJECTS:

- VUT-junior project 2018: “Wollastonite: synthesis and processing of porous scaffolds through 3D-printing”.
- VUT-junior project 2019 in collaboration with the Faculty of Civil Engineering (FAST): “Synthesis, processing and characterization of advanced BaO-MgO-Al_2O_3-SiO_2 system, as a candidate for near-future thermal and environmental barrier coatings”.
- VUT-junior project 2019: “Characterization and degradation assessment of magnesium-based biomaterials under physiological conditions”.